



# High-throughput coating with biodegradable antimicrobial pullulan fibres extends shelf life and reduces weight loss in an avocado model

Huibin Chang<sup>1,4</sup>, Jie Xu<sup>2,4</sup>, Luke A. Macqueen<sup>1</sup>, Zeynep Aytac<sup>2</sup>, Michael M. Peters<sup>1</sup>, John F. Zimmerman<sup>1</sup>, Tao Xu<sup>2</sup>, Philip Demokritou<sup>1,2,3</sup> and Kevin Kit Parker<sup>1</sup>

**Food waste and food safety motivate the need for improved food packaging solutions. However, current films/coatings addressing these issues are often limited by inefficient release dynamics that require large quantities of active ingredients. Here we developed antimicrobial pullulan fibre (APF)-based packaging that is biodegradable and capable of wrapping food substrates, increasing their longevity and enhancing their safety. APFs were spun using a high-throughput system, termed focused rotary jet spinning, with water as the only solvent, allowing the incorporation of naturally derived antimicrobial agents. Using avocados as a representative example, we demonstrate that APF-coated samples had their shelf life extended by inhibited proliferation of natural microflora, and lost less weight than uncoated control samples. This work offers a promising technique to produce scalable, low-cost and environmentally friendly biodegradable antimicrobial packaging systems.**

Each year, microbial contamination accounts for more than 600 million cases of foodborne illness and 420,000 deaths worldwide<sup>1</sup>, with at least US\$17.6 billion in economic cost due to foodborne illness in the United States alone<sup>2</sup>. Active antimicrobial food packaging systems, with release kinetics tailored to inhibit microbial proliferation<sup>3,4</sup>, have the potential to simultaneously reduce foodborne illnesses and spoilage, while saving money in lost revenue. Although antimicrobial films/coatings have been developed that can help reduce contamination<sup>5,6</sup>, they are often limited by poor release kinetics, requiring the use of large quantities of active ingredients<sup>7,8</sup>. For example, antimicrobial zein films released essential oil but only initially reduced bacterial counts<sup>7</sup>. In parallel with these efforts, biodegradable materials and environmentally friendly processing methods are also desired<sup>9</sup>. Collectively, the development of sustainable food packaging materials to enhance food safety and quality has become a major societal priority.

Fibrous materials are an attractive alternative to films for producing antimicrobial food packaging systems because their high surface-to-volume ratios allow for more efficient release of antimicrobial agents. This means that fibrous polymers have the potential to reduce the quantity of antimicrobial agents used to achieve food safety, while minimizing harm to the organoleptic properties of foods. Electrospinning is one of the most popular techniques for fabricating micro/nanofibres for food packaging applications<sup>10</sup>. Electrospun antimicrobial zein-based composite nanofibres in minuscule quantities were reported to reduce *Escherichia coli* and *Listeria innocua* populations after 24 h of exposure<sup>11,12</sup>. However, due to low production rates<sup>11</sup> and the requirement for high-voltage electrical fields electrospinning has yet to gain practical applications in food packaging.

These challenges motivated us to develop a cost-effective and high-throughput fibre-based food packaging system capable of

rapidly wrapping food. In this study, we introduce an approach to antimicrobial packaging that directly coats food products with non-toxic, biodegradable antimicrobial fibres. We use a high-throughput system, termed focused rotary jet spinning (FRJS)<sup>13</sup>, to produce antimicrobial fibres containing naturally derived antimicrobial agents. To achieve direct packaging onto food, we use water as the only solvent and pullulan as the fibrous backbone. Pullulan is a naturally occurring extracellular polysaccharide that is generally regarded as safe (GRAS) by the US Food and Drug Administration<sup>14</sup>. Using this process, we show that antimicrobial packaging can be produced in an environmentally safe and sustainable manner. To validate this approach, antimicrobial pullulan fibres (APFs) were deployed against common food pathogens such as *E. coli*, *L. innocua* and *Aspergillus fumigatus*, and produced a reduction in bacterial and fungal populations. Additionally, we demonstrate that APFs can be directly deposited on avocados to extend their shelf life through inhibiting proliferation of microorganisms and reducing weight loss. Using avocados as a proof of concept, these results indicate that FRJS-produced APFs offer a promising approach to produce scalable, low-cost and environmentally friendly antimicrobial food packaging systems.

## Results

**Direct coating of avocados with pullulan fibres.** To achieve direct coating of fresh food products, FRJS was used to manufacture pullulan fibres (PFs) with water as the only solvent. Using FRJS, fibres can be conformally deposited onto a target surface by using centrifugal force to push dissolved polymer solutions through a small orifice in a spinneret to form fibres and utilizing a focused air stream to control fibre deposition (Fig. 1a and Supplementary Fig. 1)<sup>13</sup>. Here we used FRJS to synthesize PFs and directly deposit these fibres onto the surface of avocados in a layer-by-layer fashion to form a

<sup>1</sup>Disease Biophysics Group, John A. Paulson School of Engineering and Applied Sciences, Harvard University, Boston, MA, USA. <sup>2</sup>Center for Nanotechnology and Nanotoxicology, Department of Environmental Health, Harvard T. H. Chan School of Public Health, Harvard University, Boston, MA, USA. <sup>3</sup>Nanoscience and Advanced Materials Center, Environmental Occupational Health Sciences Institute, School of Public Health, Rutgers Biomedical Health Sciences, Piscataway, NJ, USA. <sup>4</sup>These authors contributed equally: Huibin Chang, Jie Xu. ✉e-mail: [pdemokri@hsph.harvard.edu](mailto:pdemokri@hsph.harvard.edu); [kkparker@seas.harvard.edu](mailto:kkparker@seas.harvard.edu)

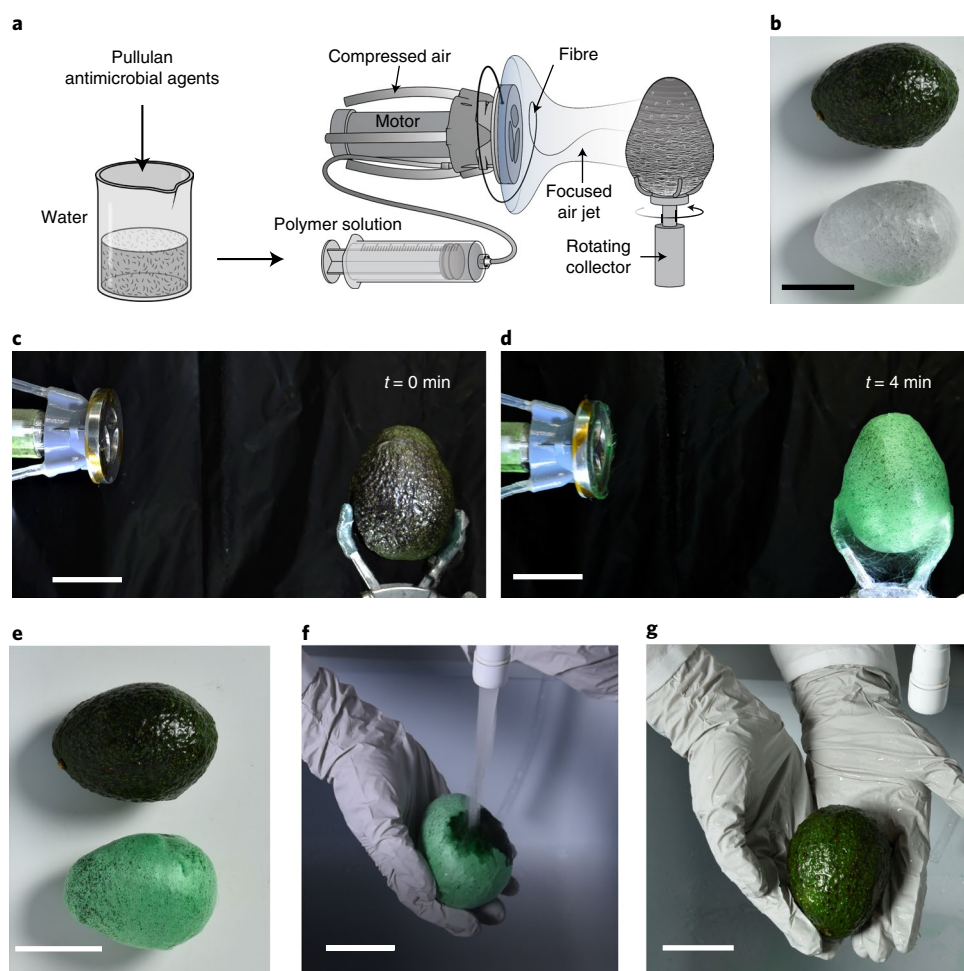


**Fig. 1 | Direct coating of avocados with rinsible PFs.** **a**, Schematic of the FRJS fibre spinning system. **b**, Avocado with and without PF coating. **c,d**, Set-up of FRJS before (**c**) and after (**d**) PF coating. **e**, The colour of the PFs can be changed by adding food dye. **f**, Removal of the coating by rinsing with water. **g**, Avocado after PF coating removal. Scale bars, 5 cm.

stable coating (Fig. 1b). Avocados were selected as an exemplar fruit in this study because they are prone to post-harvest deterioration, including uneven ripening and decay<sup>15</sup>, making them a suitable candidate for testing this direct coating approach to food packaging.

Using FRJS, the entirety of an avocado could be coated in 2–4 min with no further processing required, as shown in Fig. 1c,d and Supplementary Video 1. First, individual PFs were obtained by applying a heat gun near the spinneret to quickly evaporate water solvent during fibre formation (Supplementary Fig. 2). Next, as an initial test to determine if these PFs could act as a carrier system for various antimicrobial agents, a green food dye was incorporated into the polymer solution. This yielded a bright green fibre coating (Fig. 2d–f), suggesting a capacity for carrying antimicrobial agents, while also providing visual decoration that may be of consumer interest. This packaging was easily removed as shown in Fig. 1e,f and Supplementary Video 2: rinsing in water for at least 20 s resulted in complete dissolution of the PFs. Additionally, PFs were also completely degraded in soil after 3 d (Supplementary Fig. 3a). We also tested chemically crosslinked PFs in soil and, as expected, observed a relatively slower degradation rate (>14 d) than that of pure PFs (Supplementary Fig. 3b).

**Morphological and physicochemical characterization of APFs.** We investigated whether PFs could act as a carrier system for antimicrobial agents, without disrupting fibre formation or subsequent

fibre morphology. To test this, APFs were synthesized that incorporated naturally derived antimicrobial agents<sup>11</sup>, namely, thyme oil (1%, w/v), citric acid (5%, w/v) and nisin (0.005%, w/v). To confirm that these dopants caused minimal morphological changes, PFs and APFs were examined by scanning electron microscopy (SEM) (Fig. 2a,c). This revealed similar morphology for both conditions (Fig. 2b,d) with fibre diameters of  $1.4 \pm 0.7 \mu\text{m}$  and  $1.5 \pm 0.6 \mu\text{m}$  for PFs and APFs, respectively, suggesting that the incorporation of antimicrobial agents into the PFs had minimal effect on the fibre formation process. Additionally, the specific surface area, average pore diameter and total pore volume of PFs and APFs determined by Brunauer–Emmett–Teller (BET) surface area analysis (Supplementary Table 1) are similar. This further indicates that the fibre formation process was not disrupted by the addition of antimicrobials.

Given these minimal changes in morphology, we sought to ensure that antimicrobial agents were successfully incorporated into APFs using Fourier transform infrared spectroscopy (FTIR) (Fig. 2e). For PFs, the characteristic peaks between  $1,500$  and  $650 \text{ cm}^{-1}$  for pullulan were observed, with accompanying C–O stretches at  $1,130$ – $1,180 \text{ cm}^{-1}$  and  $1,070$ – $1,090 \text{ cm}^{-1}$ , which were consistent with previous literature reports<sup>16</sup>. For APFs, the presence of each antimicrobial ingredient was observed in the spectra, with characteristic peaks at  $\sim 1,721 \text{ cm}^{-1}$  belonging to the C=O stretch of citric acid and the characteristic peak at  $1,653 \text{ cm}^{-1}$  belonging to amide groups of

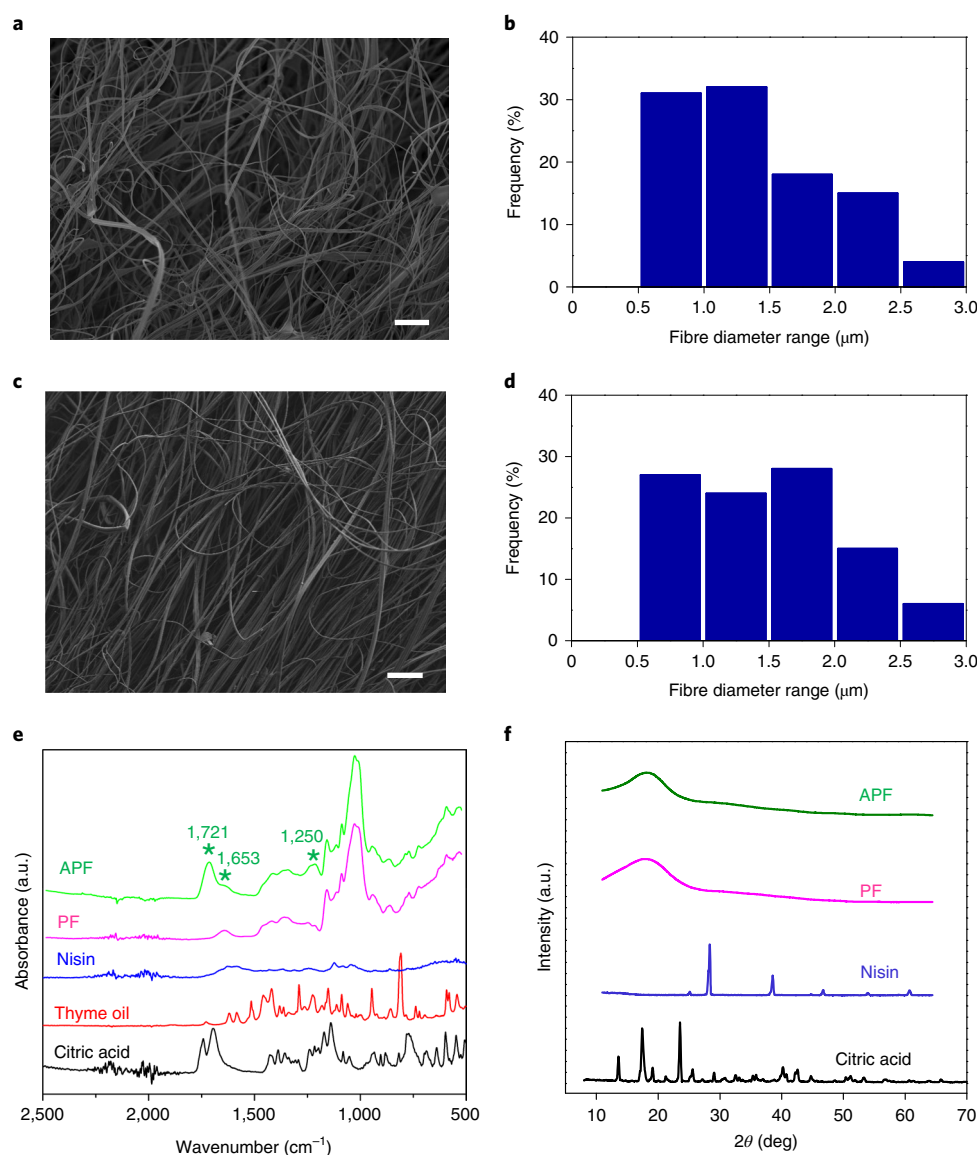


**Fig. 2 | Morphology and chemical composition of PFs and APFs.** **a–d**, Representative SEM images of PFs (**a**) and APFs (**c**), and histograms of the distribution of fibre diameters ( $n=100$ ) for PFs (**b**) and APFs (**d**). Scale bars, 20 μm. **e**, FTIR spectra of PFs and APFs with corresponding reference spectra for thyme oil, citric acid and nisin, indicating their inclusion in APFs. Asterisks represent FTIR peaks at 1,721, 1,653 and 1,250  $\text{cm}^{-1}$ . **f**, X-ray diffraction pattern of PFs, and APFs, with reference peaks for crystalline nisin and citric acid, indicating minimal crystalline domains in the fibrous materials.

nisin<sup>11,17</sup>. Thyme oil is less well resolved but exhibited characteristic peaks at 1,627, 1,360, 1,250 and 800  $\text{cm}^{-1}$ , due to the aromatic C–C stretching, isopropyl group, C–O stretching and aromatic C–H bending vibrations, respectively<sup>18</sup>. This suggested that the resulting peak observed at 1,250  $\text{cm}^{-1}$  in the spectra of APFs belonged to the vibrational C–O stretch of thyme oil. In summary, C–O vibration of thyme oil at 1,250  $\text{cm}^{-1}$ , C–O stretching of citric acid at 1,721  $\text{cm}^{-1}$  and amide groups of nisin at 1,653  $\text{cm}^{-1}$  suggested the incorporation of these antimicrobial agents into APFs.

To confirm that these antimicrobial components were well distributed throughout the body of the fibre, we then performed X-ray diffraction to check for the presence or absence of crystalline domains, which could indicate incomplete dissolution (Fig. 2f). Nisin and citric acid displayed their characteristic crystalline peaks, while PFs and APFs displayed broad peaks at  $2\theta=10\text{--}25^\circ$ , which are characteristic of amorphous polymers. This confirmed that crystalline domains were not present inside the fibres, suggesting that the

antimicrobial agents were likely to be uniformly dissolved throughout the body of the fibres.

**Antimicrobial and antifungal efficacy of APFs.** To assess the antimicrobial and antifungal efficacy of APFs, fibre substrates were put into tight contact with *E. coli* ( $\sim 5 \log$  colony-forming unit (CFU) per sample), *L. innocua* ( $\sim 5 \log$  CFU per sample) and *A. fumigatus* ( $\sim 3 \log$  CFU per sample) for 5 min, 1 h and 24 h periods using a direct contact assay method<sup>11</sup> (Fig. 3a). Here, aluminium foil and PFs without antimicrobial agents were used as controls, with fibres coated at a surface density of 2.5  $\text{mg cm}^{-2}$ . The antimicrobial and antifungal efficacy of APFs is summarized in Fig. 3b–d, with fold changes in inhibition being normalized by the initial sample concentrations (on aluminium foil after 5 min contact time). As shown, APFs achieved an  $\sim 2$  and  $\sim 5 \log$  CFU  $\text{ml}^{-1}$  population reduction of *E. coli* after 5 min and 1 h of contact time, respectively (Fig. 3b), while the aluminium foil substrate and PF controls showed minimal

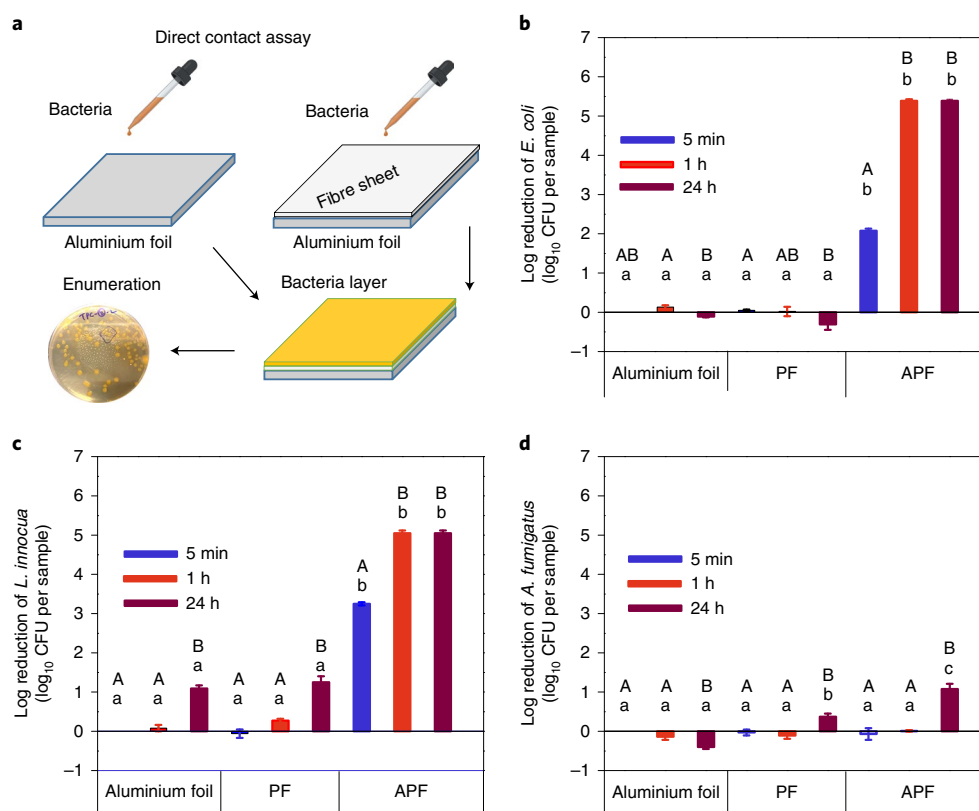


**Fig. 3 | Direct contact assay of antimicrobial and antifungal activity of APFs.** **a**, Schematic of the direct contact assay. **b–d**, *E. coli* (**b**), *L. innocua* (**c**) and *A. fumigatus* (**d**) were directly contacted with aluminium foil, PFs and APFs ( $2.50 \text{ mg cm}^{-2}$ ) on a  $2 \times 2 \text{ cm}^2$  area and incubated at  $37^\circ\text{C}$  for 5 min, 1 h and 24 h.  $n = 3$ ; error bars indicate s.e.m. Data in the same material group labelled with different upper-case letters are significantly different ( $P < 0.05$ ). Data in the same contact time group labelled with different lower-case letters are significantly different ( $P < 0.05$ ).

influence on the growth of *E. coli*. For *L. innocua* (Fig. 3c), a 3.25 and  $\sim 5$  log reduction was obtained after 5 min and 1 h of contact time with the APFs, respectively. It was also notable to see that both PFs and aluminium foil controls resulted in  $\sim 1$  log reduction of *L. innocua* after 24 h of contact time. In terms of antifungal efficacy, a  $\sim 1$  log CFU  $\text{ml}^{-1}$  population reduction of *A. fumigatus* was obtained for APFs after 24 h of contact time (Fig. 3d). Similarly, aluminium foil and PF controls had no impact on the growth of fungal spores, with a less than 1 log population fluctuation after 24 h of contact time. Taken together, this indicated that the inclusion of antimicrobial agents can lead to substantial reduced levels of contamination by microorganisms, in turn leading to enhanced food safety and potentially reduced food spoilage and extended viable storage times.

#### Effect of APF coating on the preservation and quality of avocados.

To assess whether APFs can reduce food spoilage, we measured the number of rotten avocados among the APF, PF and uncoated experimental groups after 7 d of storage at  $22^\circ\text{C}$  (Fig. 4a,b). Packaging with a fibre surface density of  $5.0 \text{ mg cm}^{-2}$  was used due to lower weight loss and higher antimicrobial activity compared with fibre coating of  $2.5 \text{ mg cm}^{-2}$  as shown in Supplementary Figs. 5 and 6. APF coatings were able to reduce the percentage of rotten avocados from 90% to 50% over a 7 d storage period (Fig. 4c). The uncoated and PF-coated avocados started to visibly decay by day 7 and visible rotten areas were observed on 90% of the avocados (Fig. 4d,e). In contrast, only 50% of APF-coated avocados showed obvious rotting (Fig. 4f). The weight loss and the natural microflora on the exocarp of avocado were measured as shown in Fig. 4g,h. APF-coated avocados displayed less weight loss and the least amount of natural microflora after 7 d in comparison with the uncoated and PF-coated

avocados. We note that the natural microflora level of the PF-coated avocados was lower than that of the control on day 7, which may have resulted from natural microflora colony differences among avocados, or from the physical barrier caused by fibre coating or the potential removal of microflora from the exocarp before recovery.

To determine how APF density might preserve fruit over time, metrics of avocado quality were quantitatively defined as weight loss, natural microflora, colour change, pH and firmness (Fig. 5 and Supplementary Figs. 5–7). Two groups of avocados coated with different surface densities of APFs ( $2.5$  and  $5.0 \text{ mg cm}^{-2}$ ) were prepared. The weight loss and natural microflora in two cases were also measured. As shown in Supplementary Fig. 5, both groups of APF-coated avocados show less weight loss than the control, but the fibre density has a minimal effect on weight loss. For total aerobic bacteria (Supplementary Fig. 6a,c), both groups of APF-coated avocados showed a lower amount of total aerobic bacteria than the control starting at day 4. A relatively larger reduction of total aerobic bacteria was observed with higher surface density ( $5.0 \text{ mg cm}^{-2}$ ) than with  $2.5 \text{ mg cm}^{-2}$  at day 11. For yeasts and moulds (Supplementary Fig. 6b,d), higher APF density resulted in lower amounts of yeasts and moulds, which is more obvious in the earlier period (days 4 and 7). In summary, a higher density of APFs is more efficient at inhibiting the population of natural microflora and fungi.

To assess discolorations in the avocados, the exocarp and mesocarp were measured for shifts in green discoloration (Fig. 5a–c and Supplementary Fig. 7) based on the CIELAB colour space<sup>19</sup>, where  $a^*$  is used as a measure of colour preservation (green value). During the first 4 d of storage, a sharp shift in exocarp  $a^*$  was observed, indicating a discoloration of the avocado from green. After the



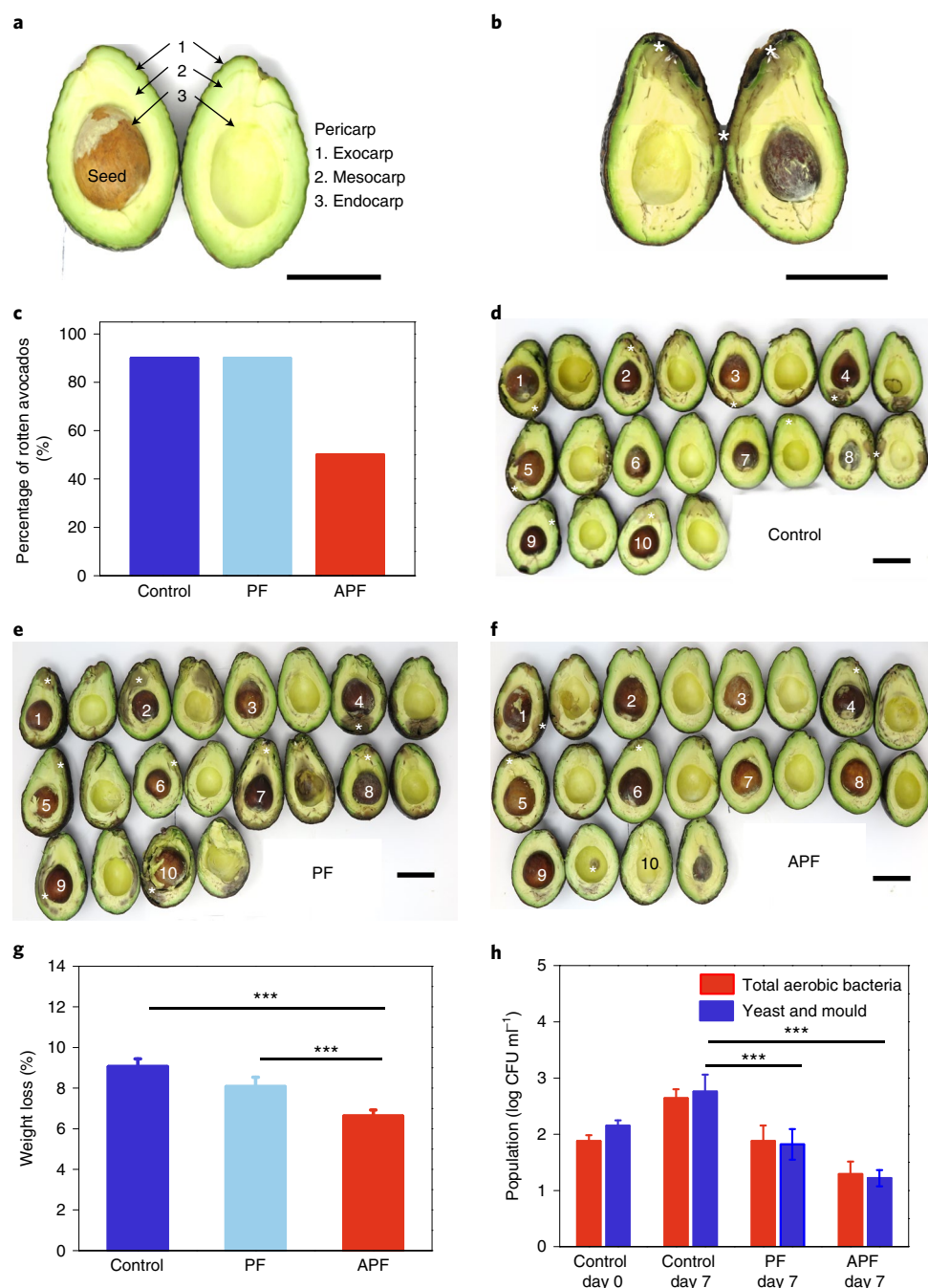


**Fig. 4 | Effect of APF coating ( $5.0 \text{ mg cm}^{-2}$ ) on avocado rotting.** **a**, Diagram of avocado. **b**, Representative rotten mesocarp areas of avocados indicated by asterisks. **c**, Percentage of rotten avocados after storage at  $22^\circ\text{C}$  for 7 d under various fibre coating conditions. Ten avocados were examined for each of the three conditions (control with no coating, PFs, APFs) as shown in **d–f** at day 7. **d–f**, Images of cut avocados from the uncoated control group (**d**), the PF group (**e**) and the APF group (**f**). Areas of mesocarp rotting are indicated by white asterisks. Scale bars, 5 cm. **g**, Weight loss of avocados ( $n=10$  avocados). **h**, Natural microflora (total aerobic bacteria, yeast and mould) of avocados at day 0 and day 7.  $n=3$  avocados. All error bars are s.e.m. Data labelled with \*\*\* are significantly different ( $P < 0.05$ ).

initial shift, minimal discoloration of the exocarp was observed, both in the presence or absence of APF coatings. With respect to mesocarp discoloration, APF-coated avocados displayed lower  $a^*$  than uncoated controls, indicating a preservation of the avocados' internal green coloration, which was also consistent across different fibre surface densities ( $2.5$  versus  $5.0 \text{ mg cm}^{-2}$ ).

The firmness and pH change of avocados with and without APF coating were also measured during storage (Fig. 5d–g). The mesocarp displayed a rapid decline in firmness over a 4 d storage

period, whereas no notable changes were noted in the exocarp. We observed that APF-coated avocados did not show notable differences in the degree of firmness compared with the control samples, regardless of fibre surface density (Fig. 5d,e). With regards to pH, avocados with APF coatings show a difference, with the exocarp yielding a lighter acidity, probably because of miniscule amounts of citric acid present on the surface (Fig. 5f,g). However, mesocarp pH was maintained at natural levels, with no difference between coating and control samples.

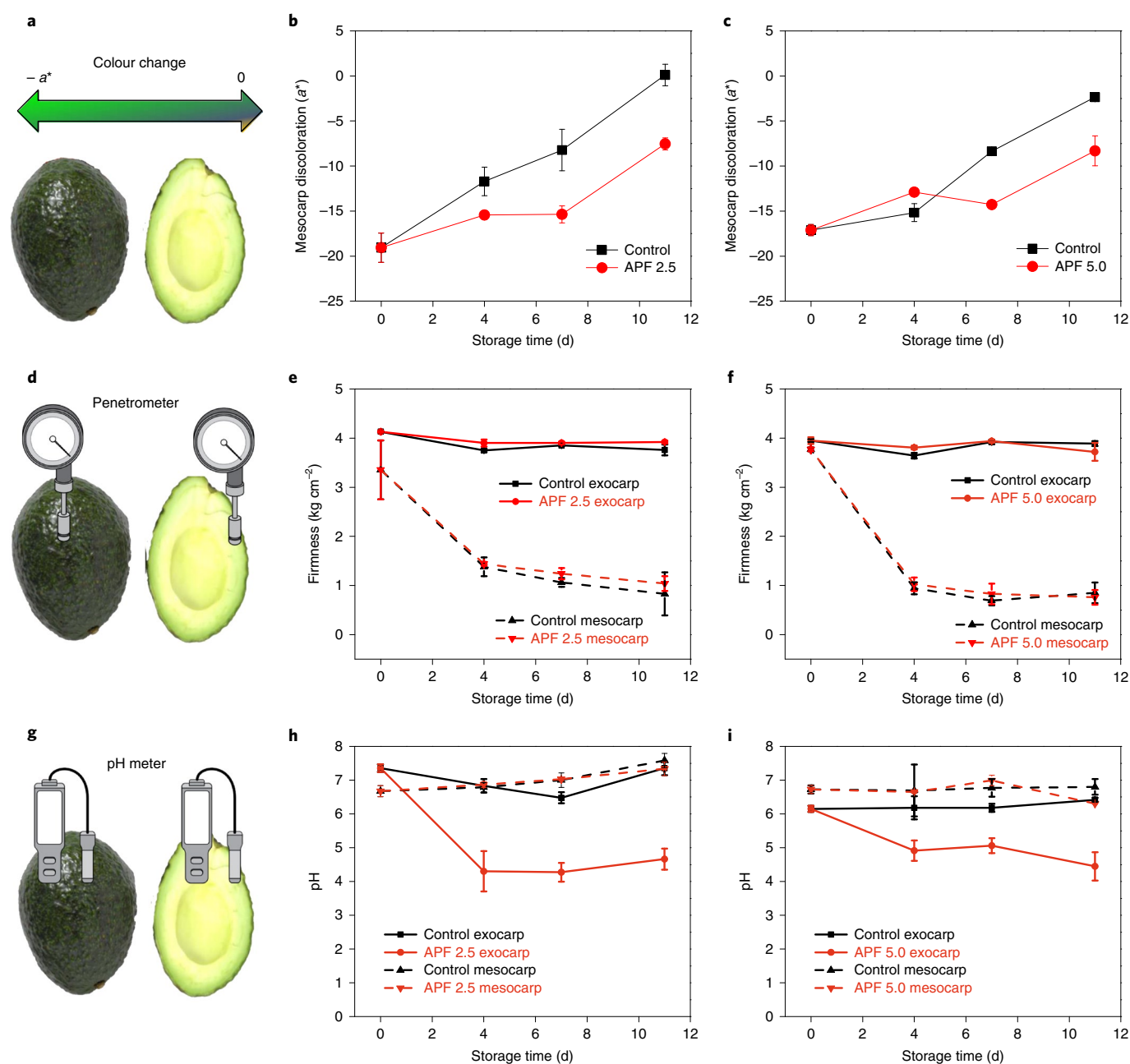


**Fig. 5 | The effect of APF coating on avocado colour, firmness and pH during storage at 22°C. a–c,** Exocarp discoloration as denoted by  $a^*$ : schematic (a) and change in discoloration with APF coatings of 2.5  $\text{mg cm}^{-2}$  (b) and 5.0  $\text{mg cm}^{-2}$  (c). **d–f,** Firmness of mesocarp and exocarp: schematic (d) and change in firmness with APF coatings of 2.5  $\text{mg cm}^{-2}$  (e) and 5.0  $\text{mg cm}^{-2}$  (f). **g–i,** pH of mesocarp and exocarp: schematic (g) and change in pH with APF coatings of 2.5  $\text{mg cm}^{-2}$  (h) and 5.0  $\text{mg cm}^{-2}$  (i). Control, avocados without fibre coating.  $n = 3$  and three areas were measured for each avocado. All error bars are s.e.m.

### FRJS-produced APFs in active food packaging applications.

Active antimicrobial food packaging systems are a promising approach to enhance safety and extend the shelf life of foods<sup>4,20</sup>. To date, the use of micro/nanofibres for food packaging has been limited due to the low experimental throughput and their reliance on non-GRAS materials and chemical processes. This study demonstrates a scalable fibre spinning system for sustainable food packaging technology that enables the one-step synthesis and direct coating of antimicrobial fibres onto fresh foods without further treatment. In FRJS, centrifugal force is used to form fibres while compressed air is used to control fibre deposition, which is distinct from other fibre production methods such as solution blow spinning where compressed air is used for both fibre formation and deposition

processes. In addition, the scalability of the FRJS-based approach is evident from the higher pullulan fibre production rate (0.2  $\text{g min}^{-1}$ ) compared with electrospinning (0.01  $\text{g min}^{-1}$ )<sup>21</sup>. Therefore, FRJS can potentially be used directly in the field to deposit antimicrobial packaging onto fresh foods. FRJS can also be used at various other critical control points from farm to fork to package food substrates to enhance their food safety and quality.

With respect to environmental effects, pullulan is an attractive biopolymer for biodegradable food packaging applications<sup>16,22–24</sup>. Our study shows that PFs are dissolved in liquid environments and biodegraded in the soil environment. It is worth noting that chemically crosslinked PFs degrade more slowly than pure PFs (Supplementary Fig. 3). The commercial use of these materials for

food packaging has been hampered by high costs (ranging from US\$25 to US\$30 kg<sup>-1</sup>)<sup>25</sup>. Here, micro/nanofibre-based coating, with its high surface-to-volume ratio, has allowed us to achieve effective antimicrobial activities using only limited surface treatments, with surface densities of 5.0 mg cm<sup>-2</sup>. This suggests that fresh fruits, such as avocado, can be coated with antimicrobial fibres inexpensively (for only a few cents per fruit), even without accounting for further cost reductions when scaling up production. The concern for environmental effect also extends to the selection of antimicrobial agents, polymers and organic solvents used in the synthesis process. In this case water was used as a solvent to synthesize fibres from a non-toxic, GRAS, biodegradable polymer.

In regard to food safety, fresh fruits and vegetables, such as avocados<sup>26,27</sup> and apples<sup>28</sup>, can be contaminated with pathogens during post-harvest processing. This suggests a need for improved food packaging, which can be rapidly deployed to protect against a wide range of potential contaminants. Here, APFs were shown to have broad antimicrobial and antifungal functionality by incorporating multiple naturally derived agents. The successful incorporation of these naturally derived antimicrobials in APFs is evident in the FTIR spectra as shown in Fig. 2e. Additionally, we confirmed the high surface-to-volume ratio of APFs using BET surface data analysis (Supplementary Table 1). These data suggested that reduced quantities (5.0 mg cm<sup>-2</sup>) of APFs should be sufficient to inactivate pathogens compared with film-based packaging systems. More specifically, APFs showed a strong antimicrobial efficacy against Gram-negative and Gram-positive bacteria (Fig. 3b,c). Compared with conventional techniques such as dip coating to preserve avocados<sup>29</sup>, APF coatings show a similar result: both antimicrobial packaging methods can prolong shelf life under ambient conditions for up to 7 d. Additionally, APFs also offer a strong antifungal efficiency, with the population of *A. fumigatus* being substantially reduced (>90%) after a 24 h contact time. Fungal spoilage is often considered a more challenging problem to address, with fewer studies having reported efficient antifungal food packaging systems, especially in fibre form<sup>30,31</sup>. In addition, APFs may be recommended to reduce spoilage during transportation, where simple rinsing can be used to remove the packaging before consumption.

The effects of APFs on shelf life were also explored and APFs can substantially reduce the percentage of rotten avocados compared with the control and PF-coated avocados (Fig. 4). This suggests the ability of APFs to reduce decay can primarily be attributed to the addition of antimicrobial agents in the PFs. For avocados, post-harvest disease is common and is believed to be the result of bacterial contamination, resulting in further degradation<sup>32</sup>. As shown in Fig. 4f and Supplementary Fig. 5, the natural microflora of avocados coated with APFs were persistently lower than those of the control samples, suggesting that bacteria were unable to initiate this infiltration process, thereby reducing the natural decay of avocados. Additionally, reductions in the natural microflora on the exocarp may also reduce the chance for surface-to-surface cross-contamination, further potentiating gains in food safety and quality. It is worth noting that to assess pathogen populations on avocado exocarp, we inoculated avocados with precise numbers of pathogens and thereby accurately estimated fold-reduction with or without APF coatings.

To test the practical applications of APFs, APF-coated avocados were stored in the refrigerator. Although the majority of APF coatings are fibrous structures, we observed that some fibrous coatings in the contact areas started to dissolve on day 3 and gradually changed to a transparent layer due to water accumulation either from metabolic activity or humidity in the refrigerator. An additional layer of crosslinked PF coating on the avocados can improve the durability of the fibre coating but need a longer rinse time to remove (Supplementary Fig. 8).

## Conclusions

Fibre-based active food packaging systems have recently gained increased attention due to their potential to enhance food safety and quality. Here, a scalable, sustainable and cost-effective approach, FRJS, has been deployed to synthesize environmentally friendly and rinsible PFs containing naturally derived antimicrobial agents. Such fibres can be directly coated on food substrates (for example, avocado). The APFs show high antimicrobial efficacy against food pathogens such as *E. coli* and *L. innocua*. In a case study with avocados, APF coatings were shown to be able to reduce the percentage of rotten avocados and resulted in lower natural microflora populations, less weight loss and reduced discoloration of the mesocarp during storage. The water-based synthesis process, the edible and washable nature of pullulan, and high-throughput fibre technology combine to present a promising method to package perishable food products to enhance food safety and quality while reducing food waste.

## Methods

**Materials.** Pullulan (lot number 0E2732, Hayashibara) was purchased from DKSH North American. Sodium trimetaphosphate (lot number SLCD1552), sodium hydroxide (NaOH, pellets) and active agents including citric acid (251275-100 G, lot number MKCH1340), nisin (N5764-5G, lot number 019M4063V) and thyme oil (W3066509-1KG-K, lot number MKCJ4106) were purchased from Sigma-Aldrich. Food Colour and egg dye were purchased from McCormick.

**Direct coating of food substrates with FRJS.** FRJS was used for fibre production as shown in Supplementary Fig. 1. The FRJS system itself consists of a high-speed motor spindle, a custom-made spinneret to extrude polymer solutions, a syringe pump (lot number 703007, Harvard Apparatus) to transfer precursor solutions to the spinneret, a three-dimensionally printed air blower with three air nozzles to focus the ejected fibre stream, and a stand to hold the motor and spinneret in place. A motor running at a speed of ~200 r.p.m. was used to rotate the food substrate, avocados, during fibre coating to ensure uniform deposition across the food surface. Additionally, a heat gun (Stein HL1502S) was used to rapidly evaporate water from the PFs before their impact with the food substrate, thereby ensuring efficient PF production. The custom-made spinneret was constructed from stainless steel and contained three orifices (diameter, 400 µm) drilled into the side walls to allow for the extrusion of polymer solutions while under rotation<sup>13</sup>.

An aqueous solution of pullulan and a cocktail of antimicrobial agents was prepared for the synthesis of APFs. Various pullulan concentrations ranging from 10% to 30% (w/v) were used as part of a parametric analysis to synthesize the fibres. The antimicrobials used here were composed of three agents: 1% (w/v) thyme oil, 5% (w/v) citric acid and 0.2% nisin mixture (w/v, 0.005% pure nisin)<sup>11</sup>. The solutions were then loaded in a plastic syringe (60 ml BD Luer-Lock tip) and the syringe pump was used to transfer solutions to the spinneret. PFs were deposited on the collection mandrel or directly onto avocados, and the mass per surface area was adjusted by varying the collection time.

After a systematic investigation of each parameter, the final parameters used to spin continuous PFs were as follows: 20% (w/v) pullulan solution in water, 1 ml min<sup>-1</sup> solution flow rate, 10,000 r.p.m. spinneret rotation speed, 0.2 MPa compressed air flow, and a 15–20 cm distance between spinneret and collector. To make chemically crosslinked PFs, sodium trimetaphosphate was added into the pullulan solution at 0.5 wt% of pullulan polymer and then mixed for at least 2 h. Before spinning, 10 wt% NaOH aqueous solution was added at a volume ratio of 1:10 (NaOH/pullulan solution) to activate crosslinking<sup>13</sup>. The spinning parameters were the same as for pure pullulan solution. To cover an avocado with fibres at 2.5 and 5 mg cm<sup>-2</sup> takes about 2 and 4 min, respectively.

**Morphology and physicochemical characterization of fibres.** Fibre samples were mounted on a stub using double-sided carbon tape and then coated with Pt/Pd (Denton Vacuum) to minimize charging. Fibre morphology was observed by scanning electron microscopy (Zeiss FESEM Ultra Plus). The average diameter of fibres was measured from scanning electron microscopy images using ImageJ Software ( $n = 100$ ).

The specific surface area (m<sup>2</sup> g<sup>-1</sup>) of fibres, the average pore radius (nm) and the total pore volume (cm<sup>3</sup> g<sup>-1</sup>) were investigated by BET analysis (Quantachrome NOVA touch LX4). Before the analysis, fibres were degassed in cells at 323.15 K for 12 h. Low-temperature (77.35 K) nitrogen adsorption isotherms were then obtained at relative pressures from 0.005 to 1.00.

The FTIR spectra of the fibres and antimicrobial agents were measured using attenuated total reflectance–FTIR spectroscopy (Lumos, Bruker). For each sample, the recorded spectrum was collected from a total of 32 scans.

The inclusion of nisin and citric acid in the PFs was investigated by X-ray diffraction (Bruker D2 Phaser) in the 2θ range of 8–0°. Due to the liquid state at room temperature, X-ray diffraction was not performed for the thyme oil.



**Biodegradability test.** To evaluate the biodegradability of the PFs in soil, a soil degradation test was performed in organic soil (100% organic soil, Organic Plant Magic) containing 10% v/v water. Four fibrous sheets ( $\sim 0.5 \times 2 \text{ cm}^2$ ) were cut and stored on the surface of organic soil in a Petri dish at 22 °C. The dimensions of the PF sheets were recorded daily to assess their biodegradability.

**Antimicrobial efficacy of APFs against food-related microorganisms.** *Strain information.* *E. coli* ATCC 25922, *L. innocua* ATCC 33090 and *A. fumigatus* ATCC 96918 were used in these studies as representatives of Gram-negative and Gram-positive microorganisms, and fungus, respectively.

*E. coli* and *L. innocua* were resuscitated and streak plated from the stock and maintained on tryptic soy agar (TSA; Hardy Diagnostic) at 4 °C. A single colony from TSA was transferred into 10 ml of tryptic soy broth (Hardy Diagnostic). After incubation at 37 °C for 24 h, bacterial broth was centrifuged at 1,462g for 20 min (Allegra 6R, Beckman Coulter). After discarding the supernatant, 2 ml phosphate-buffered saline (PBS 1×) buffer was used to resuspend the pellet. The cell density was adjusted to  $\sim 10^8 \text{ CFU ml}^{-1}$  by PBS. Freeze-dried *A. fumigatus* was rehydrated in sterile deionized water and further transferred onto malt extract agar (MEA) and incubated at 30 °C for 3 d. To produce spores, single colonies were further transported onto MEA and incubated at 30 °C for 7 d until the conidia became dark green. Mature spores were harvested from the lawn and then diluted with deionized water. The final concentration of spores was about  $\sim 10^7$  measured by a manual hemocytometer (Diagnocine).

**Direct contact assay.** To test the antimicrobial efficacy of fibres, 100 µl of bacterial culture was diluted in a 10 ml agar slurry (0.85% NaCl, 0.3% agar). Inoculated agar slurry (300 µl) was transported onto a  $2 \times 2 \text{ cm}^2$  fibre sheet placed onto a similar sized piece of aluminium foil as a substrate (Fig. 3a). After a contact time of 5 min, the agar slurry formed a gel layer with a thickness of less than 1 mm. The treated fibre sheets were then placed in an incubator and further contacted with the bacterial gel for 1 h or 24 h. To maintain gel hydration, an open water reservoir was placed in incubator to keep the relative humidity at  $\sim 80\%$ . Since aluminium foil was used as a substrate to deposit the fibres, the bacteria survivors on aluminium foil and PFs without antimicrobial agents were used as controls. The population reduction shown in Fig. 3 was the absolute population difference from the starting concentration of bacteria or fungus on aluminium foil with 5 min contact time.

**Enumeration.** After the desired exposure time, each test fibre sheet together with aluminium foil substrate was transferred into a sterile Whirl-Pak bag with 2.7 ml of PBS to reach a 10-fold dilution. Then, the sample bag was homogenized inside a Stomacher bag (Whirl-Pak™ sterile sampling bag, Nasco) for 2 min at a normal speed. The elute was then serially diluted to a proper level. For *E. coli* and *L. innocua*, 100 µl of proper dilution was pour plated onto TSA and incubated at 37 °C for 24 h. For *A. fumigatus*, 100 µl of proper dilution was pour plated onto MEA and incubated at 30 °C for 48 h.

**Statistical analysis of antimicrobial efficacy testing.** Three independent replicates were conducted for each condition. The number counts of *E. coli*, *L. innocua* and *A. fumigatus* were converted into log CFU per sample. Statistical analyses to illustrate differences within the same materials and within the same contact time were performed by one-way analysis of variance within the confidence interval of 95% ( $P < 0.05$ ) (SPSS Statistics for Windows, v.19.0, IBM).

**Shelf-life study of APF-coated avocados.** *Sample preparation.* Hass avocados were purchased from local stores on the same day each experiment was performed. We selected avocado samples of similar colour, size, shape, firmness and with no obvious bruises or fungal infections by visual observation. Avocados were transported to the laboratory in paperboard boxes with support to avoid mechanical damage. All avocados were grouped and labelled properly before further usage.

**Avocado coating and storage.** PFs with and without antimicrobial agents were directly deposited on the avocados. During this process, avocados were held and rotated using a clamp and motor system, enabling a uniform fibre coating across the entire avocado surface; surface density ( $\text{mg cm}^{-2}$ ) was controlled by coating time. The surface density of each fibre sheet was adjusted to 2.5 or  $5.0 \text{ mg cm}^{-2}$  by measuring the weight and area of fibre sheets.

After coating, all avocados were stored in a board box at room temperature (22 °C) with a relative humidity of  $\sim 30\%$ . The experimental design of the avocado shelf-life study is illustrated in Supplementary Fig. 4. To obtain the percentage rotting rate, 10 avocados from each of the control, PF ( $5.0 \text{ mg cm}^{-2}$ ) and APF ( $5.0 \text{ mg cm}^{-2}$ ) groups were used and withdrawn on day 0 (the day the coating was applied) and day 7. The natural microflora and weight loss of each group was analysed. For the remaining test parameters (weight loss, colour change, firmness and pH), three avocados from the control and APF ( $2.5$  and  $5.0 \text{ mg cm}^{-2}$ ) groups were used. Sample analysis was conducted on days 0, 4, 7 and 11. On each analysis date, three avocados were randomly selected from each group and the PF or APF coatings were removed gently by hand to avoid bruising. The data from three independent samples were used.

To test the practical applications of PFs, PF-coated avocados and chemically crosslinked PF-coated avocados were stored in a refrigerator ( $\sim 4$  °C and  $50\% \pm 5\%$

humidity). The fibre-coated avocados were digitally photographed with a camera every day to assess the durability of the fibre coatings.

**Natural microflora analysis.** For natural microflora analysis, each avocado was put into a 500 ml Stomacher bag, mixed with 100 ml of maximum recovery diluent and hand massaged gently for 2 min. The solution was then serially diluted and plated on selective media plates. The following categories of microorganisms were analysed: total aerobic bacteria, yeast and mould. For total aerobic bacteria, diluted samples were enumerated on plate count agar and incubated at 35 °C for 2 d. For yeast and mould, diluted samples were enumerated on plate count agar (acidified with 10% tartaric acid to pH 3.5) and incubated at room temperature (22 °C) for 5 d. To reach the detection limit of  $10 \text{ CFU ml}^{-1}$ , 1 ml of solution from the Stomacher bag was separated onto three plates and the total numbers of colonies from the three plates were combined and reported.

To assess the effect of APF surface density on the natural microflora of avocados, fibre coatings with two different surface densities ( $2.5$  and  $5.0 \text{ mg cm}^{-2}$ ) were studied separately. To ensure APF-coated, PF-coated and uncoated control samples are under the same experimental conditions, uncoated control samples are used for each set of experiments.

**Quality analysis.** For quality analysis, the weight, colour (exocarp and mesocarp), pH (exocarp and mesocarp) and firmness (exocarp and mesocarp) of avocados were measured as a function of storage time. Before analysis, the PFs on the surface of coated avocados were manually rubbed away until no observable fibre remained.

The percentage of rotting avocados was calculated from equation (1):

$$\text{percentage of rotting avocados (\%)} = \frac{n_{\text{rotted}}}{n} \times 100 \quad (1)$$

where  $n_{\text{rotted}}$  is the number of avocados defined as rotted and  $n$  is the total number of avocados tested (here,  $n = 10$ ). An avocado was regarded as rotted when there was an area of decay observed on the cut regions, regardless the decay size.

For weight measurements, avocados were weighed using an Ohaus SCOUT balance scale. The weight of all avocados from each group on different days was measured. The weight loss on each measured day is expressed by equation (2):

$$\text{weight loss (\%)} = \frac{\text{weight}_{\text{day 0}} - \text{weight}_{\text{day } x}}{\text{weight}_{\text{day 0}}} \times 100 \quad (2)$$

Colour analysis of the avocados was achieved by photographing each avocado using a digital camera (Canon PowerShot G1X; 50 mm lens; aperture,  $f/4.0$ ; exposure time,  $1/125 \text{ s}$ ; ISO, 400) in a light tent with controlled lighting (two light-emitting diode lights; daylight balanced at 5,600 K). Three representative marked areas of each avocado picture were segmented, and the average RGB values were calculated by ImageJ (NIH). The RGB values were then transformed into  $a^*$  values (greenness) by using the CIELAB colour space to define the green–red axis. After cutting the avocado in half, an image of the mesocarp of each avocado was captured and analysed in the same manner.

The exocarp pH of avocados was measured with a pH meter and a flat-head pH probe (Sper Scientific). For exocarp pH, 100 µl of neutral deionized water (pH 7.3) was placed on each marked circular area ( $\sim 2 \text{ mm}$  diameter) on the surface of each avocado before measurement. The pH probe was pressed onto the liquid droplet and the pH value was recorded. After cutting the avocado in half, the mesocarp pH was also measured in the same manner. Three representative locations of each avocado were selected for both exocarp and mesocarp pH measurement.

Avocado firmness was measured with a fruit sclerometer (Beslands). During the measurement, the fruit sclerometer was placed perpendicular to the measurement surface and evenly pressed into the avocado. When the test head reached the scale line (10 mm), the measurement was recorded as the firmness of the avocado. Avocado firmness is expressed in  $\text{kg cm}^{-2}$ . Exocarp firmness was measured by placing the fruit sclerometer on the avocado surface. After cutting the avocado in half, mesocarp firmness was measured on the cut side in a similar manner. Three representative locations were measured for each avocado, separately for exocarp or mesocarp.

For statistical comparisons of weight loss and natural microflora, a one-way analysis of variance was performed to determine statistically significant differences between the groups. Statistical significance was assumed with a  $P < 0.05$  for all tests. We then used an *F*-test to determine differences in variances. For groups that possessed equal variances, we performed a *t*-test with two samples assuming equal variance. All statistical analyses were performed using Microsoft Excel v.2111 with the Analysis ToolPak.

**Reporting summary.** Further information on research design is available in the Nature Research Reporting Summary linked to this article.

## Data availability

The data that support the findings of this study are available from the corresponding authors upon reasonable request. Source data are provided with this paper.



Received: 2 September 2021; Accepted: 28 April 2022;  
Published online: 20 June 2022

## References

- Lee, H. & Yoon, Y. Etiological agents implicated in foodborne illness world wide. *Food Sci. Anim. Resour.* **41**, 1–7 (2021).
- Hoffmann, S. & Ahn, J.-W. Economic cost of major foodborne illnesses increased \$2 billion from 2013 to 2018. *Amber Waves* (2 April 2021).
- Vilela, C. et al. A concise guide to active agents for active food packaging. *Trends Food Sci. Technol.* **80**, 212–222 (2018).
- Sharma, R., Jafari, S. M. & Sharma, S. Antimicrobial bio-nanocomposites and their potential applications in food packaging. *Food Control* **112**, 107086 (2020).
- Mellinas, C. et al. Active edible films: current state and future trends. *J. Appl. Polym. Sci.* **133**, 42631 (2016).
- Marelli, B., Brenckle, M., Kaplan, D. L. & Omenetto, F. G. Silk fibroin as edible coating for perishable food preservation. *Sci. Rep.* **6**, 1–11 (2016).
- Göksen, G., Fabra, M. J., Ekiz, H. I. & López-Rubio, A. Phytochemical-loaded electrospun nanofibers as novel active edible films: characterization and antibacterial efficiency in cheese slices. *Food Control* **112**, 107133 (2020).
- Wen, P. et al. Fabrication of electrospun polylactic acid nanofilm incorporating cinnamon essential oil/ $\beta$ -cyclodextrin inclusion complex for antimicrobial packaging. *Food Chem.* **196**, 996–1004 (2016).
- Jafarzadeh, S. et al. Biodegradable green packaging with antimicrobial functions based on the bioactive compounds from tropical plants and their by-products. *Trends Food Sci. Technol.* **100**, 262–277 (2020).
- Bhushani, J. A. & Anandharamakrishnan, C. Electrospinning and electrospinning techniques: potential food based applications. *Trends Food Sci. Technol.* **38**, 21–33 (2014).
- Aytac, Z. et al. Development of biodegradable and antimicrobial electrospun zein fibers for food packaging. *ACS Sustain. Chem. Eng.* **8**, 15354–15365 (2020).
- Aytac, Z. et al. Enzyme- and relative humidity-responsive antimicrobial fibers for active food packaging. *ACS Appl. Mater. Interfaces* **13**, 50298–50308 (2021).
- Chang, H. et al. Structure–function in helical cardiac musculature using additive textile manufacturing. Preprint at *bioRxiv* <https://doi.org/10.1101/2021.08.18.456852> (2021).
- Agency Response Letter, GRAS Notice No. GRN 000099 (US Food and Drug Administration, 2002).
- Munhuwey, K., Mpai, S. & Sivakumar, D. Extension of avocado fruit postharvest quality using non-chemical treatments. *Agronomy* **10**, 212 (2020).
- Karim, M. R. et al. Preparation and characterization of electrospun pullulan/montmorillonite nanofiber mats in aqueous solution. *Carbohydr. Polym.* **78**, 336–342 (2009).
- Niaz, T. et al. Polyelectrolyte multicomponent colloidosomes loaded with nisin Z for enhanced antimicrobial activity against foodborne resistant pathogens. *Front. Microbiol.* **8**, 2700 (2018).
- Trindade, G. G. G. et al. Carvacrol/ $\beta$ -cyclodextrin inclusion complex inhibits cell proliferation and migration of prostate cancer cells. *Food Chem. Toxicol.* **125**, 198–209 (2019).
- Durmus, D. CIELAB color space boundaries under theoretical spectra and 99 test color samples. *Color Res. Appl.* **45**, 796–802 (2020).
- Abdollahzadeh, E., Nematollahi, A. & Hosseini, H. Composition of antimicrobial edible films and methods for assessing their antimicrobial activity: a review. *Trends Food Sci. Technol.* **110**, 291–303 (2021).
- Poudel, D. et al. Novel electrospun pullulan fibers incorporating hydroxypropyl- $\beta$ -cyclodextrin: morphology and relation with rheological properties. *Polymers* **12**, 2558 (2020).
- Xiao, Q. & Lim, L.-T. Pullulan–alginate fibers produced using free surface electrospinning. *Int. J. Biol. Macromol.* **112**, 809–817 (2018).
- Tomasula, P. M. et al. Electrospinning of casein/pullulan blends for food-grade applications. *J. Dairy Sci.* **99**, 1837–1845 (2016).
- Li, R. et al. Electrospinning pullulan fibers from salt solutions. *Polymers* **9**, 32 (2017).
- Farris, S., Unalan, I. U., Introzzi, L., Fuentes-Alventosa, J. M. & Cozzolino, C. A. Pullulan-based films and coatings for food packaging: present applications, emerging opportunities, and future challenges. *J. Appl. Polym. Sci.* **131**, 40539 (2014).
- Willingham, S. L. et al. Effects of rootstock and nitrogen fertiliser on postharvest anthracnose development in Hass avocado. *Australas. Plant Pathol.* **35**, 619–629 (2006).
- Hartill, W. F. T. & Everett, K. R. Inoculum sources and infection pathways of pathogens causing stem-end rots of ‘Hass’ avocado (*Persea americana*). *NZ J. Crop Hortic. Sci.* **30**, 249–260 (2002).
- Angelo, K. et al. Multistate outbreak of *Listeria monocytogenes* infections linked to whole apples used in commercially produced, prepackaged caramel apples: United States, 2014–2015. *Epidemiol. Infect.* **145**, 848–856 (2017).
- Le, K. H. et al. A novel antimicrobial ZnO nanoparticles-added polysaccharide edible coating for the preservation of postharvest avocado under ambient conditions. *Prog. Org. Coat.* **158**, 106339 (2021).
- Topuz, F. & Uyar, T. Antioxidant, antibacterial and antifungal electrospun nanofibers for food packaging applications. *Food Res. Int.* **130**, 108927 (2020).
- Feng, K. et al. Enhancement of the antimicrobial activity of cinnamon essential oil-loaded electrospun nanofilm by the incorporation of lysozyme. *RSC Adv.* **7**, 1572–1580 (2017).
- Garcia, F. & Davidov-Pardo, G. Recent advances in the use of edible coatings for preservation of avocados: a review. *J. Food Sci.* **86**, 6–15 (2021).
- Shi, L., Le Visage, C. & Chew, S. Y. Long-term stabilization of polysaccharide electrospun fibres by in situ cross-linking. *J. Biomater. Sci. Polym. Ed.* **22**, 1459–1472 (2011).

## Acknowledgements

We thank the Nanyang Technological University–Harvard T. H. Chan School of Public Health Initiative for Sustainable Nanotechnology for funding support (project number NTUHSPPH 18003). This work was performed in part at the Center for Nanoscale Systems (CNS), a member of the National Nanotechnology Coordinated Infrastructure Network (NNCI), which is supported by the National Science Foundation under NSF award number 1541959 and at the Harvard MRSEC (grant numbers DMR-1420570 and DMR-2011754).

## Author contributions

K.K.P. and P.D. supervised the research. K.K.P., P.D., H.C., J.X. and L.A.M. designed the study. H.C., J.X., Z.A. and M.M.P. conducted the experiments and analysed the data. L.A.M., T.X. and J.E.Z. provided support to perform experiments and data analysis. All authors discussed the results and contributed to the writing of the final manuscript.

## Competing interests

Harvard University filed for intellectual property relevant to this manuscript, listing K.K.P., P.D., H.C. and L.A.M. as inventors. The remaining authors declare no competing interests.

## Additional information

**Supplementary information** The online version contains supplementary material available at <https://doi.org/10.1038/s43016-022-00523-w>.

**Correspondence and requests for materials** should be addressed to Philip Demokritou or Kevin Kit Parker.

**Peer review information** *Nature Food* thanks Feng Jiang, Long Yu and the other, anonymous, reviewer(s) for their contribution to the peer review of this work.

**Reprints and permissions information** is available at [www.nature.com/reprints](http://www.nature.com/reprints).

**Publisher's note** Springer Nature remains neutral with regard to jurisdictional claims in published maps and institutional affiliations.

© The Author(s), under exclusive licence to Springer Nature Limited 2022